

Chapter 8

High-Power RF systems: 201.25 and 402.5 MHz

8.1 Introduction to rf Systems

The rf systems for the buncher and the cooler are required to match the muon beam into the longitudinal acceptance of the cooling channel and to replenish the beam energy lost during ionization cooling. Since they must operate inside the strong solenoid fields they must be normal conducting. These systems require a large number of rf cavities operating at high gradient, and a large amount of pulsed rf power. They are technically challenging and expensive, and have therefore been the focus of continued development during Study-II. The cooling channel layout has continued to evolve since Study-I, with emphasis on integration of realistic components into the available space along with optimization of the channel performance. The buncher and cooling channel systems must accommodate liquid-hydrogen absorbers, high-gradient rf cavities, windows, tuners, superconducting solenoids, diagnostics, pumping, harmonic cavities and other equipment. The system must be designed in such a way as to allow assembly and access for maintenance. The buncher and cooling channel comprises a large number of modules (cells). The cell layouts are described in Section 8.4. Each module contains two or four 201.25 MHz closed-cell cavities and is powered by one or two high-power multibeam klystrons. The density of equipment in the building is therefore high and the systems must be carefully laid out to allow access for installation and maintenance. Following the cooling channel is a matching section containing rf and solenoids, but no absorbers.

The proposed buncher, cooling channel, and matching section is approximately 183 m long and requires 184 cavities and 84 klystrons at 201.25 MHz and an additional 6 cavities

8.2. NCRF Specifications for Buncher and Cooling

and 3 klystrons at 402.5 MHz. The total installed power is approximately 780 MW (≈ 1.56 MW average), and the installed voltage is 1080 MV.

The cooling channel is followed by an acceleration section employing 299 two-cell superconducting rf cavities operating at 201.25 MHz. These structures are also challenging because of the high gradient and large physical size. Peak power requirements for the acceleration section are not as high as for the normal conducting rf sections, but the pulse length is much longer. Many superconducting cavities can be powered from a single klystron station. Several multi-cell rf cavities may share a common cryostat. The final energy at the end of the accelerating section is 20 GeV, compared with the 50 GeV of Study-I. This reduces the size and cost of the acceleration section significantly.

8.2 NCRF Specifications for Buncher and Cooling Channels

Table 8.1 summarizes the inventory of normal conducting rf cavities (NCRF). The cooling channel simulations were based upon ideal pillbox cavities with lengths determined by the space available in the chosen lattices (and zero space between cavities). The gradients and phases of these cavities were adjusted to optimize the cooling channel performance while keeping the gradients and rf power requirements within feasible limits. Table 8.2 shows the peak cavity power and klystron output power to meet these requirements, and the total power for each cavity type. Both tables also show how the required voltages are obtained using realistic re-entrant or “omega” shaped cavities with closed-off irises of finite thickness. The loss of active length in the realistic case is compensated by the greater efficiency of the rounded design. To be conservative, the iris diameter used for the omega cell was sufficient to accommodate any reasonable beryllium foil. In practice, the foils may be smaller and in any case will decrease in size towards the end of the cooling channel. Ideally, the cavity shape would be optimized for each foil size. This would maximize the efficiency and minimize the power cost. Note that the rf power requirements are dominated by the cooling sections (1,1)-(1,3) and (2,1)-(2,3), which have the largest number of cavities and the highest gradients.

8.3 RF Station Description

Each rf station consists of a modulator for two klystrons, a distribution system, and low-level rf and controls driving two or more cavities. The modulator must provide a flat top DC pulse of up to 125 μs with a recharge time of less than 20 ms. (This is equivalent to

Table 8.1: Parameters for the ideal (pillbox) and practical (omega) NCRF cavities.

*Note: Kilpatrick number is about 15 MV/m at 201.25 MHz.

Ideal pillbox dimensions used in the simulations (see Chapter 5)						
Section	Radius (m)	Length (m)	Freq. (MHz)	No. of cavities	E_{pk}^* (MV/m)	V_{eff} (MV)
b1	0.570	0.373	201.25	4	6.40	2.07
b2	0.570	0.373	201.25	8	6.00	1.94
b3	0.570	0.373	201.25	8	8.00	2.59
(1,1)-(1,3)	0.570	0.466	201.25	68	15.48	5.76
(2,1)-(2,3)	0.570	0.559	201.25	74	16.72	6.71
match	0.570	0.559	201.25	22	16.72	6.71
b1 402.5 MHz	0.285	0.186	402.5	2	6.40	1.03
b2 402.5 MHz	0.285	0.186	402.5	4	8.00	1.29
Omega cavities						
Section	Radius (m)	Length (m)	Freq. (MHz)	No. of cavities	E_{pk}^* (MV/m)	V_{eff} (MV)
b1	0.607	0.405	201.25	4	7.41	2.07
b2	0.607	0.405	201.25	8	6.95	1.94
b3	0.607	0.405	201.25	8	9.27	2.59
(1,1)-(1,3)	0.607	0.405	201.25	68	20.62	5.76
(2,1)-(2,3)	0.615	0.483	201.25	74	23.06	6.71
match	0.615	0.483	201.25	22	23.06	6.71
b1 402.5 MHz	0.308	0.288	402.5	2	6.57	1.03
b2 402.5 MHz	0.308	0.288	402.5	4	8.21	1.29

a repetition rate of 50 Hz, but not every 50 Hz pulse is required. The output from the AGS appears as 6 pulses spaced at 20 ms followed by a 300 ms gap, with a repetition rate of 2.5 Hz.) The *average* duty factor is $\approx 1.9 \times 10^{-3}$.

Each rf station must provide approximately 10 MW of peak power to drive two cavities. The power source is a multi-beam klystron, which should give good reliability and a long operational lifetime.

Power distribution will be via high-power coaxial lines, with the power split between two or more cavities using appropriate delays to maintain the proper phase. The cavities will use coaxial feedthroughs and loop-type couplers. The high peak power requirements require careful design of the components, although the average power, of about 10 kW

8.3. RF Station Description

Table 8.2: Voltage and power requirements for the NCRF cavities.

[†] R_s , calculated, $= V^2/P$, * Real cavity, Q_0 assumed 85% of theoretical;

** Klystron forward power for 3τ filling.

Ideal pillbox							
Section	V_{eff} (MV)	R_s^{\dagger} ($M\Omega$)	P_c^* (MW)	P_{kly}^{**} (MW)	No. of cavities	P_{tot} (MW)	Sum (MW)
b1	2.07	8.899	0.567	0.628	4	2.51	
b2	1.94	8.899	0.499	0.552	8	4.42	
b3	2.59	8.899	0.886	0.982	8	7.85	
(1,1)-(1,3)	5.76	10.701	3.646	4.038	68	274.60	
(2,1)-(2,3)	6.71	11.428	4.635	5.134	74	379.91	
match	6.71	11.428	4.635	5.134	22	112.95	782.0
b1 402.5 MHz	1.03	6.275	0.200	0.222	2	0.444	
b2 402.5 MHz	1.29	6.275	0.313	0.347	4	1.387	1.8
Omega cavities							
b1	2.07	10.220	0.494	0.547	4	2.19	
b2	1.94	10.220	0.434	0.481	8	3.85	
b3	2.59	10.220	0.77	0.855	8	6.84	
(1,1)-(1,3)	5.76	10.220	3.818	4.228	68	287.54	
(2,1)-(2,3)	6.71	11.794	4.491	4.974	74	368.09	
match	6.71	11.794	4.491	4.974	22	109.43	778.0
b1 402.5 MHz	1.03	8.368	0.150	0.166	2	0.333	
b2 402.5 MHz	1.29	8.368	0.235	0.260	4	1.040	1.4

per coupler, is quite modest. Provision is made for adjusting the phase of individual cavities and for handling the reflected power during the initial part of the cavity fill time.

Each station includes a water distribution system and a rack of low-level rf hardware and controls.

8.3.1 Power Source and Equipment

The bunching, ionization cooling channel, and the match to the acceleration system requires high peak rf power sources at 201.25 MHz and 402.5 MHz to efficiently bunch, cool the muon beam and prepare it for acceleration. Table 8.2 lists the peak rf power requirements for each section. There are 184 201.25-MHz cavities in the channel that require 782 MW of rf power for a pulse length of 125 μs at 15 Hz (average) and six

402.5 MHz cavities that require 1.8 MW at 15 Hz.

An examination of the requirements shows that an rf source of about 6 or 12 MW would be ideal for the 201.25 MHz cavities and a source of 500 to 750 kW for the 402.5 MHz cavities. The rf power for the 201.25 MHz cavities could be supplied by existing gridded tubes at about the 5 MW level. However, the low gain and lifetime of gridded tubes make the R&D effort to develop an alternative most attractive. Preliminary calculations at SLAC [1] have shown that a 201.25 MHz klystron could be built with a reasonable amount of R&D. The gain, efficiency, and lifetime are all higher than a gridded tube at 50 dB, 50-70% and 50,000 hours, respectively. SLAC has examined two designs, a single-gun diode design, and a multibeam klystron (MBK). The multibeam klystron is the more attractive in that it reduces the overall length of the tube from 7.5 m to about 3.5–4.0 m. The length reduction factor of the multibeam klystron, and its potential for higher efficiency, make it the optimum candidate for the Neutrino Factory. Moreover, the length of the multibeam klystron is consistent with the manufacturing capabilities of current tube manufacturers, whereas the manufacture of a 7.5 m diode tube would be a big step and would require new and costly facility upgrades. Figure 8.1 shows a 7 beam MBK developed by Thompson for TESLA. Two such tubes have been built and tested, and have demonstrated efficiencies of 63 – 66% [2]. To provide rf power overhead for dynamic regulation of the rf phase and amplitude, a 12 MW multibeam klystron has been selected as the high-power rf source for the Neutrino Factory. This provides an rf power overhead margin of about 20% for regulation. The design will be a fully integrated horizontal package incorporating the tube, solenoid, and high-voltage terminal, as pioneered at CERN for LEP. This facilitates the replacement and installation of tubes in the facility. Another advantage of the horizontal design, besides the ease of handling, is the reduced cost of the rf building because of the lower building height requirement. With a mean-time-between-failures (MTBF) of 50,000 hours and 84 tubes, one tube will need to be replaced about every 30 days (after the initial break-in period). Since there is a comparable number of klystrons for the acceleration system, the rate of klystron failures for the facility as whole will be about two per month, on average. Many of these failures towards the end of life are gradual, and replacement can be scheduled for routine maintenance periods. Because of the large size and high cost of waveguide, the transmission lines from the tubes to the cavities will be large coaxial lines of 0.31 to 0.36 m diameter, pressurized to 1.75 atmospheres of dry air. Power splitters divide the rf power from each tube to supply the cavities. Sections b1 and b2 of the buncher (see Chap. 5.1 and, in particular, Table 5.2) will require a 12-way splitting of the power; section b3 an 8-way split, and sections (1,1) to (2,3) of the cooling a 2-way split. Splitters with proper built-in phase delays further divide the power to each cell or cavity section of the cooling channel.

8.3. RF Station Description



Figure 8.1: Thomson TH 1801 multi-beam klystron.

The 402.5 MHz system can use currently existing 900 kW diode rf klystron amplifiers. Because of their long length, it would be advisable to fund a small R&D effort aimed to development of an integrated horizontal package for the tube. As for the multibeam klystron, this would improve the efficiency of tube handling and provide cost savings because of reduced building height requirement. Coaxial transmission lines with splitters would be used to provide the rf power to the cavities. Only 3 klystron tube amplifiers are required to supply the requirements of the 402.5 MHz buncher rf.

8.3. RF Station Description

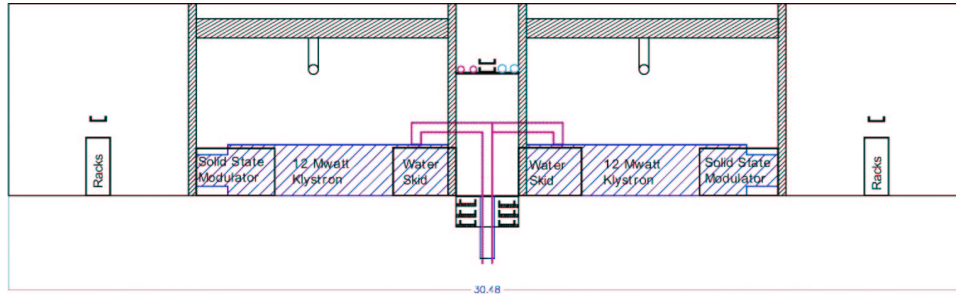


Figure 8.2: Cross section of cooling channel equipment gallery.

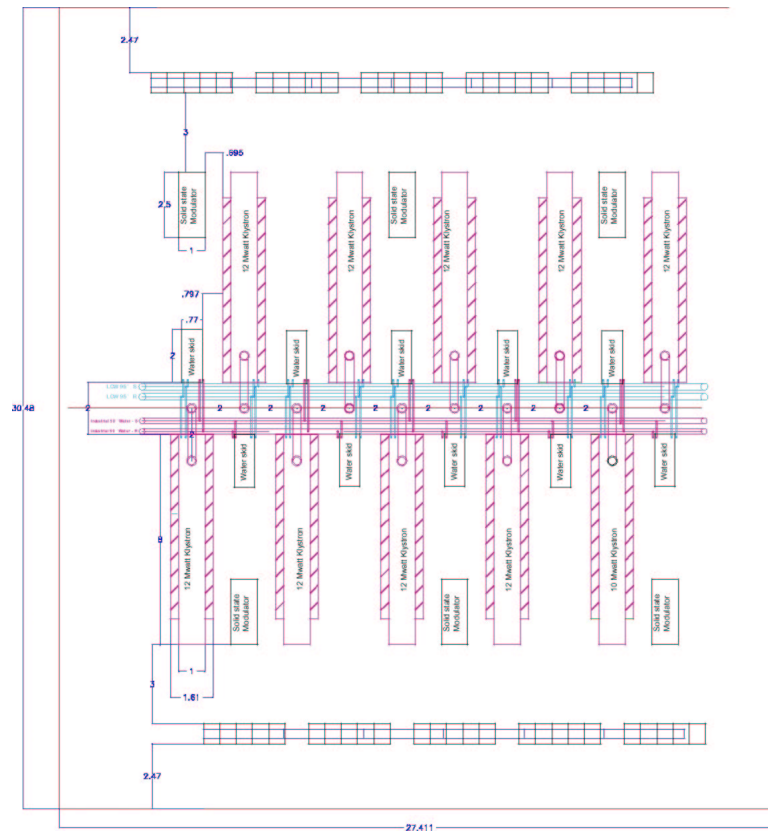


Figure 8.3: Cooling channel equipment gallery, plan view.

8.3. RF Station Description

Figures 8.2 and 8.3 show a cross section and plan view of a portion of the rf building gallery along a 201.25 MHz section. The rf building is approximately 190 m long and 30 m wide. With horizontal packaging of the 201.25 and 402.5 MHz klystrons, the height of the building roof line need only be 5.5 m. Because of the large footprint of the equipment, the klystrons are arranged side by side and on both sides of the gallery. Not shown in the figures are the transmission line splitters, required to supply the rf power to the cavities, and the utilities. The 402.5 MHz klystron system footprint will be much the same, but about half the size, and these klystrons will be located in sections b1 and b2 interspersed between the 201.25 MHz equipment.

8.3.2 Station Controls and Low-Level rf

The low-level rf (LLRF) and control system provides the drive power for the final klystron amplifier, contains feedback loops for phase, amplitude and cavity frequency control, and circuitry for personnel safety and equipment protection. A frequency reference line running the length of the complex provides an rf phasing reference to which each cavity is locked. A microprocessor in each rf station processes error information to control the amplitude and phase and thus keep the cavity tuned to the reference frequency. The microprocessor communicates with, and accepts directions from, the central control room. The system is similar to systems currently in use at Fermilab or planned for the SNS project. The LLRF system will include fast circuits to detect sparks and malfunctions and immediately inhibit the rf to protect the equipment and cavities. Other, hard-wired, fast circuits will monitor for high rf leakage from equipment or contact with high-voltage and current, and then activate interlocks for personnel protection. The equipment would be housed in five standard racks next to the klystron and associated equipment, Fig. 8.3.

8.3.3 High-Voltage Modulator and Power Supply

The high-voltage modulator and power supply for the 201.25 MHz rf system will use the latest solid-state design. Currently available Insulated Gate Bipolar Transistor (IGBT) modulator technology will be built by industry to provide the pulsed power requirements of the klystron, see Fig. 8.4. The Neutrino Factory will use IGBT modulators similar to designs currently being built for the SNS project. They are very reliable, efficient, and cost effective. A 19-beam klystron, the basis of this design, has a calculated efficiency of 70% and a klystron tube perveance of 0.5×10^{-6} . The specifications for the modulator and power supply are given in Table 8.3. The overall efficiency of the modulator and power supply from the AC mains is about 95%.

8.3. RF Station Description



Figure 8.4: Compact modulator from Diversified Technologies, Inc., Medford, MA (Capacitor bank and regulator not shown in this picture).

8.3. RF Station Description

Table 8.3: High-voltage modulator parameters.

Klystron frequency (MHz)	201.25	402.5
High-voltage (kV)	80	60
Current (A)	215	31
Duty factor (%)	0.19	0.0525
Average power (kW)	33	1.0
Voltage droop (%)	0.1	0.1

8.3.4 NCRF AC Electrical Power and Water System

The AC power for the normal conducting rf must support 84 tubes with 33 kW average power and three tubes with 1.0 kW average power, solid-state amplifiers and solenoid power supplies, cooling water systems and miscellaneous other loads. These all require a 480-V three-phase supply. In addition to this, AC power is required at 120 V and 208 V for racks and other miscellaneous equipment. This gives a total AC power requirement of 6.8 MW. Table 8.4 shows a summary of the AC power requirements.

Table 8.4: NCRF systems AC power requirements.

Item	Power (MW)
Klystron modulators (95% efficiency)	2.9
Amplifiers & supplies	1.0
Cooling + miscellaneous loads	2.3
Racks etc.	0.6
Total	6.8

The cooling water system will be sized to accommodate the average power of 6.8 MW with a proper temperature rise for safe and efficient operation of the equipment. Each klystron station requires 75 gpm of low-conductivity water (LCW) for cooling the klystron and associated equipment, and 20 gpm LCW to cool and provide temperature control of the cavity. This gives a total water requirement of 7,980 gpm. This could be divided up between room-temperature (and above) water and chilled-water systems for cavity control at 20 gpm per station. For all these systems, we assume a supply header pressure of 100 psi and return pressure of 40 psi.

8.4 Specification of NCRF Cavities for Cooling

The 201.25 MHz normal-conducting cavities in the cooling sections must operate at very high accelerating gradients. This would be impractical with conventional open-iris structures, given the large size of the beam iris required. A great improvement can be made in the shunt impedance of the cavity by closing the iris with a thin conducting barrier. This barrier must use the smallest amount of material to minimize scattering of the muon beam. In the design we close the irises with thin beryllium foils. Alternative methods of closure, such as grids of thin-walled tubes will be evaluated in the future. The foils must be thick enough to conduct away the heat from the rf currents and keep the temperature below a predetermined level. The foils are pre-stressed in tension during manufacture in order to keep them flat. This method has been tested experimentally and works well up to the point where the thermal expansion exceeds the pre-stress and the foils begin to move. Foil thicknesses have been chosen for Study-II that will keep the temperatures below this critical level. The use of tapered foils, or foils with stepped thickness, can reduce the amount of material intercepted by the core of the beam, reducing the amount of scattering significantly. Table 8.5 shows the thickness of the foils used in the simulations of the various types of cavities in the buncher and cooling channel.

The normal-conducting cavities in the buncher are the same design as those in the first cooling section, though they are operated at lower gradient, allowing the use of thinner foils. The buncher section also contains harmonic cavities operating at 402.5 MHz. These fit into the spaces that are occupied by the liquid-hydrogen absorbers in the cooling cells farther downstream. For these cavities, the foils occupy most of the diameter of the end walls, but the gradients are sufficiently low that the losses in the foils are manageable.

The normal-conducting cells must have some cooling to remove the average power losses in the walls and to stabilize the frequency. The Study-II design is based upon room temperature operation, although the option of operating at reduced temperature (*e.g.*, liquid-nitrogen temperature) has been kept open. This option would lower the wall resistance and reduce the peak power requirements, at the expense of adding an additional refrigeration system.

8.4.1 201.25 MHz Closed-Cell Description

The cooling channel simulations were based upon simple pillbox cavities that have continuous, flat, conducting end walls from the center all the way to the outer radius. The cavity lengths assumed for the simulations are just the available space divided by the appropriate number of cells. In practice the cavities must be closed by assemblies of foils or grids that are demountable to permit assembly or repair. This requires a non-

8.4. Specification of NCRF Cavities for Cooling

Table 8.5: Beryllium foil thicknesses for various cells in the buncher and cooling channel. * dual values imply a stepped-thickness foil.

Type	Section	Frequency (MHz)	Length (m)	Gradient (MV/m)	Thickness* (μm)	Radius* (cm)
end	b1	402.5	0.186	6.4	75	18
end	b2	402.5	0.186	6	75	18
end	b1	201.25	0.3728	6.4	10	21
middle	b1	201.25	0.3728	6.4	120/240	14/21
end	b2	201.25	0.3748	6	100	21
middle	b2	201.25	0.3748	6	105/210	14/21
end	b3	201.25	0.3748	8	180	21
middle	b3	201.25	0.3748	8	187/374	14/21
end	(1,1)	201.25	0.466	15.48	200/400	12/18
middle	(1,1)	201.25	0.466	15.48	700/1400	14/21
end	(1,3)-(2,1)	201.25	0.5592	16.72	248/495	12/18
middle	(1,3)-(2,1)	201.25	0.5592	16.72	917/1834	14/21
end	(2,1)	201.25	0.5592	16.72	128/256	10/15
middle	(2,1)	201.25	0.5592	16.72	495/990	12/18

zero thickness for each iris, reducing the length available for rf and lowering the effective shunt impedance. We have mitigated the losses by rounding the outer walls of the cavity to improve the quality factor and restore the shunt impedance. Any practicable assembly of foils (or grids), requires some space for flanges and access. We used a minimum spacing of 50 mm between cavities, as shown in Fig. 8.5. The dimensions of the cavities were adjusted to fit the remaining available space. Note that the resulting cavity lengths are significantly shorter than the optimum for a particle of this velocity ($\beta = 0.87$). A cavity length that is more optimal could be achieved by adjusting the total cell length appropriately and this will be done as part of the overall optimization process later. The cavity shape is slightly reentrant in order to maximize the inductance, minimize the capacitance, and, hence, get the highest shunt impedance [3]. Figures 8.5 and 8.6 show the cavities separated by a pair of foils. This allows variable thickness foils to be used where the stepped side is not exposed to rf. Figure 8.7 shows a MAFIA simulation of the electric field in two half-cells separated by a pair of foils. Some field enhancement can be seen on the noses. Alternatively, a single foil of twice the thickness could be used in the center of the iris, heated from both sides (except for the end cells). Another advantage

8.4. Specification of NCRF Cavities for Cooling

of the closed-cells is that there is no rf coupling through the iris, so the cavities can be individually phased for optimum performance of the cooling channel. One penalty of the omega shape is some field enhancement on the nose, see Figs. 8.8 and 8.9. Although the nose is made with as large a radius as practical, it still has an enhancement factor of about 1.7 over the field on axis. However, the highest surface field in Table 8.2 is only about 1.5 times the Kilpatrick number for this frequency. Furthermore, a positive aspect of this field concentration is that it is not on the foil but on the solid copper. A breakdown to this point may be less of an issue. Figure 8.9 shows the azimuthal magnetic field. The distribution on the foil, and therefore the rf heating, is similar to the pillbox model, although there is some shielding due to the noses. Figure 8.10 shows the profile of the cavity from the downstream part of the cooling channel where only two cavities are used per cooling cell (Lattice 2). The cavities are longer and closer to the optimum for this particle velocity (though there is still room for some improvement). Figures 8.11 and 8.12 show the 2D electric and magnetic field profiles for this case.

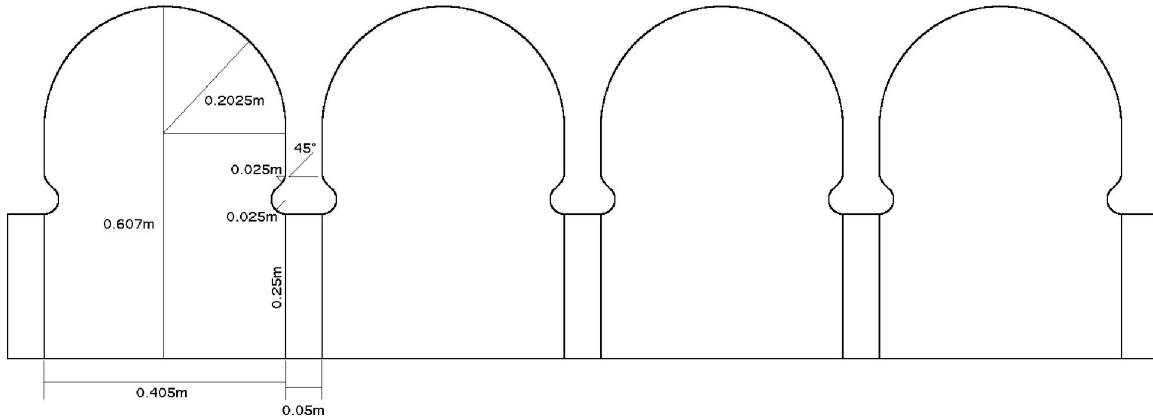


Figure 8.5: Profile of cavities for buncher and Lattice 1 cooling section.

8.4.2 Foil Requirements

The closed-cell cavity design described above assumes that beryllium foils will be used to seal off the beam irises. Other methods, including grids of thin-walled tubes, have been discussed, and show promise, but are not as far advanced in understanding or testing as the foils. Hence pre-stressed foils have been chosen as the baseline design for Study-II. The foils are made of thin high-purity beryllium sheet bonded to a thicker ring of slightly

8.4. Specification of NCRF Cavities for Cooling

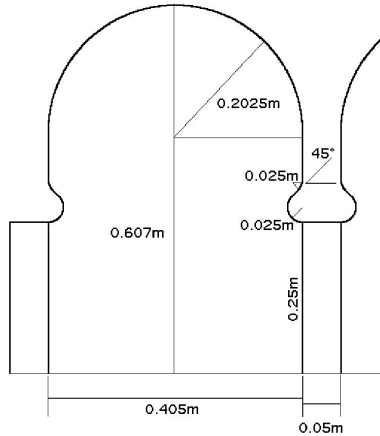


Figure 8.6: Section of one cavity.

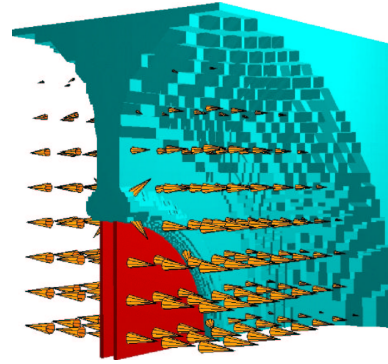


Figure 8.7: MAFIA model with two foils.

lower grade material, see Fig. 8.13. The exact details of this process are proprietary but the combination of materials used results in a small but significant difference in the thermal expansion of the foil relative to the ring assembly. This produces a tensile pre-stress on cool down from the joining operation, which helps to keep the foil flat.

When the foils are heated by rf, and only cooled by conduction to the edges, they assume an approximately parabolic temperature profile, see Fig. 8.14. The calculated rf-induced profile is slightly flatter than parabolic and can be used in ANSYS as a load set for the stress calculations. Figure 8.15 shows an example of the temperature distribution in a thin foil from such an analysis.

The foils remain flat until the thermal expansion exceeds the tensile pre-stress. At this point compressive stress is generated in the foil, and it starts to deflect by buckling into a gently bowed shape, see Fig. 8.16. The maximum allowed temperature difference is about $35\text{ }^{\circ}\text{C}$ and is approximately independent of the radius and thickness. Of course a thicker foil can take more power before reaching the buckling temperature, as shown in Fig. 8.17. A set of foils (Table 8.5), has been specified for the set of cavities used in Table 8.1, that keeps the temperatures below the critical point. For the larger irises, the foils become quite thick and the scattering of the muon beam becomes significant. One way to reduce this is to make the windows thinner in the middle, where the core of the beam passes, and thicker towards the outside, where there are fewer particles, see Fig. 8.18. It is thus possible to reduce the scattering while maintaining the same temperature rise in the foil. Figure 8.19 shows the temperature profile for a thin window of uniform thickness and for windows with thicker profiles starting at different radii. As can be seen from the

8.4. Specification of NCRF Cavities for Cooling

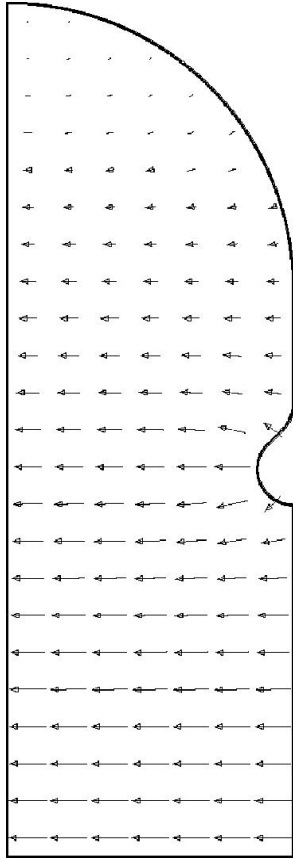


Figure 8.8: URMEL 2D E-field.

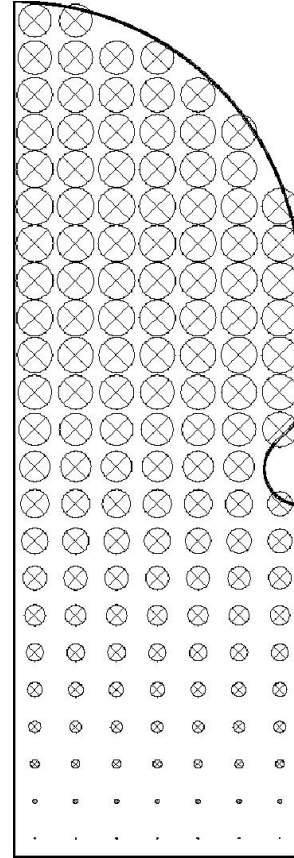


Figure 8.9: URMEL 2D azimuthal H-field.

figure, adding material at large radius has a significant effect on the temperature profile up to about one third of the way in. Beyond this point, there is diminishing return and much past halfway there is little to be gained by adding more material. Simulations have shown that such a stepped window reduces the multiple scattering significantly compared with a uniform foil for the same temperature. Going to multiple steps in thickness, or to a continuous taper, should yield further small improvements in scattering but the simulations do not show a significant improvement in transmission through the cooling channel.

The pre-stressed foil properties have been investigated experimentally in a low-power test cavity at 805 MHz using a halogen lamp as a heat source [4]. These experiments used small (160 mm diameter) foils and the results have been extrapolated to larger foils. We

8.4. Specification of NCRF Cavities for Cooling

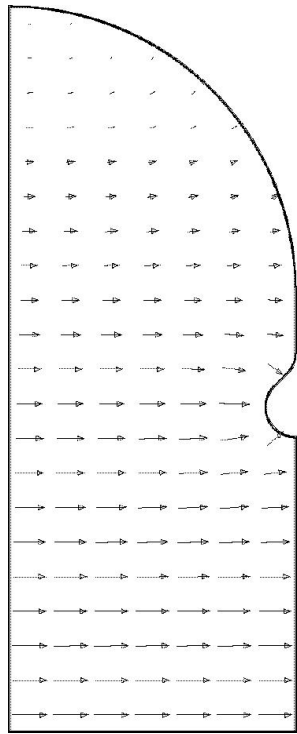


Figure 8.11: Lattice 2 cooling cavity.
URMEL 2D E-field.

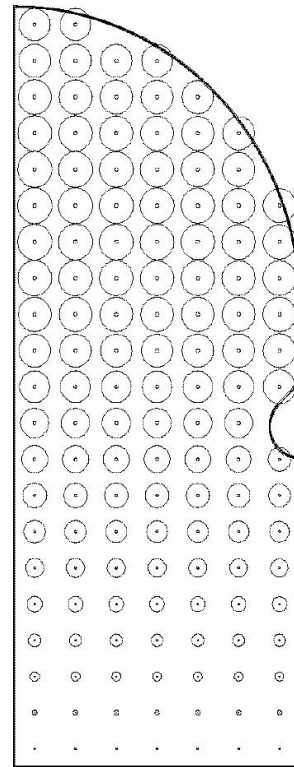


Figure 8.12: Lattice 2 cooling cavity.
URMEL 2D azimuthal H-field.

8.4. Specification of NCRF Cavities for Cooling

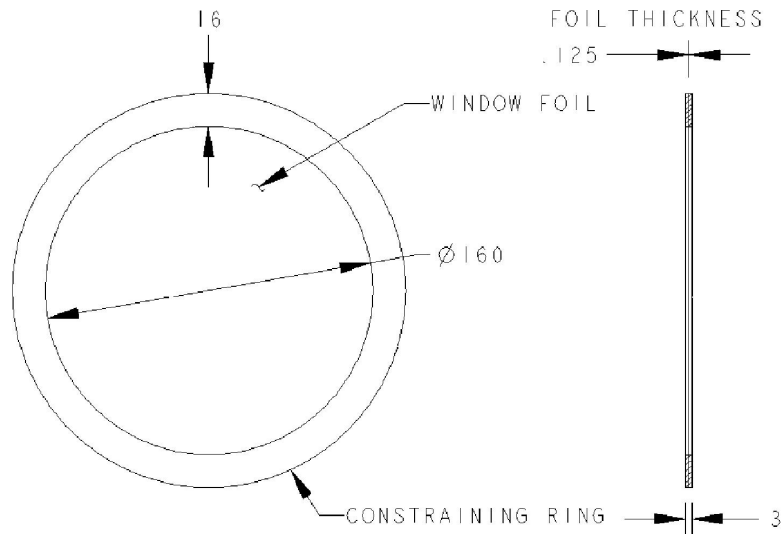


Figure 8.13: Layout of beryllium test window (all dimensions in mm).

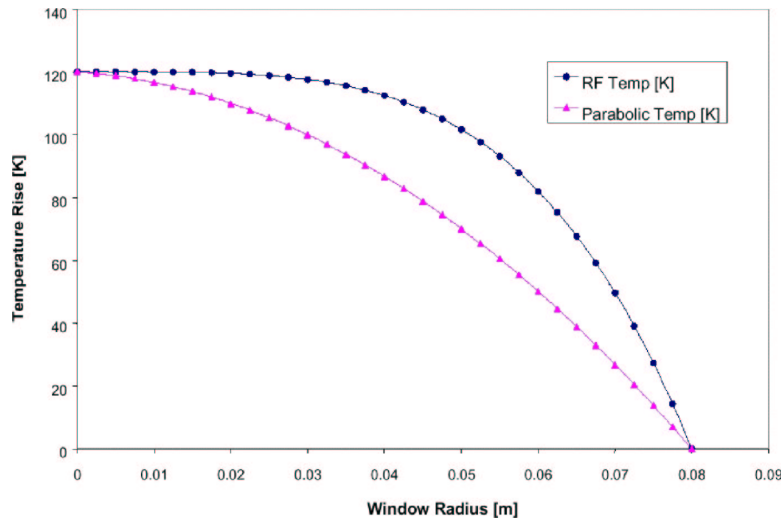


Figure 8.14: Actual temperature profile for rf heating and parabolic approximation from halogen lamp tests.

8.4. Specification of NCRF Cavities for Cooling

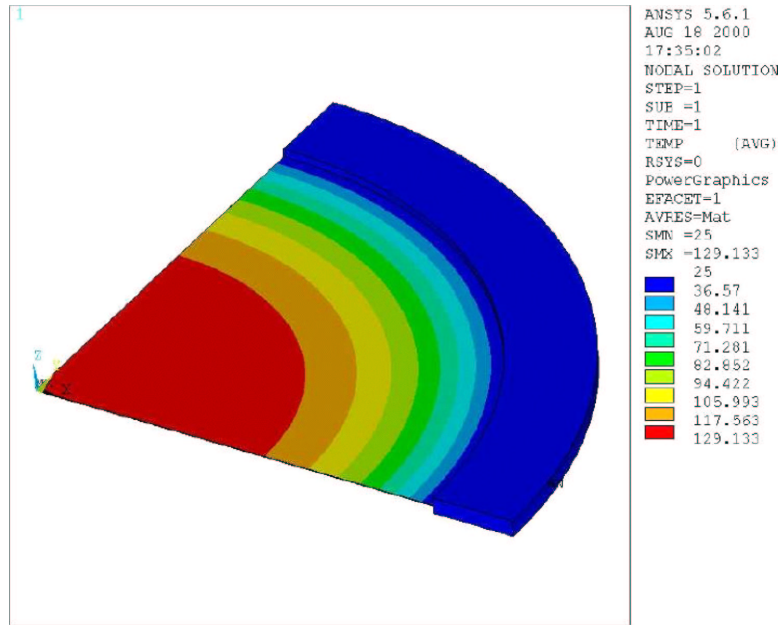


Figure 8.15: ANSYS calculated temperature profile for thin window with 60 W loading.

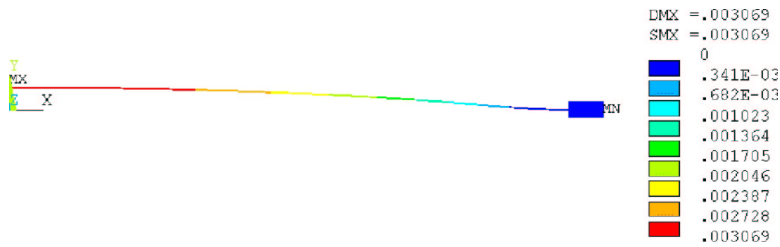


Figure 8.16: ANSYS model showing example of buckling displacement (dimensions in m).

8.4. Specification of NCRF Cavities for Cooling

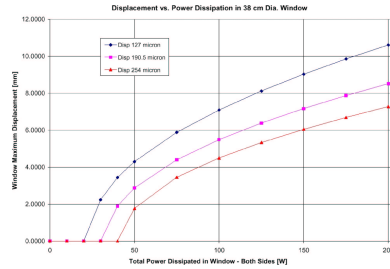


Figure 8.17: ANSYS calculated displacement *vs.* power for larger windows. The three curves represent three window thicknesses, 127 μm , 190.5 μm , and 254 μm .

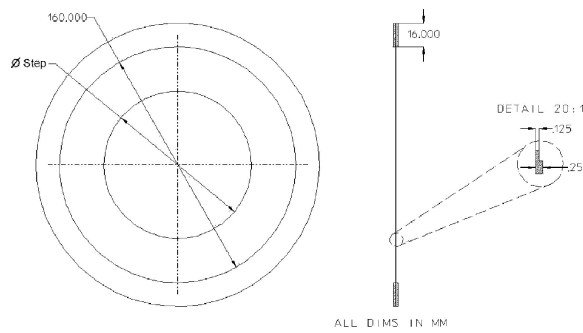


Figure 8.18: Stepped window concept.

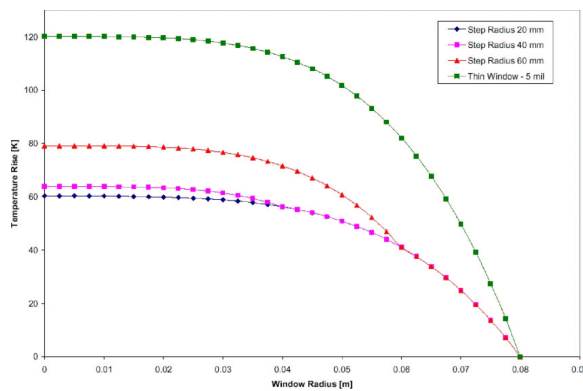


Figure 8.19: Temperature profile of uniform thin window and windows with steps to thicker outer region starting at various radii.

8.4.3 2.75 m Lattice Implementation (Lattice 1)

The cooling channel lattice is a tightly packed assembly of equipment including liquid-hydrogen absorbers, superconducting solenoids, high-gradient rf cavities, instrumentation, vacuum equipment, etc. Our studies show that it is possible to integrate all these components into the available cell length. Several iterations have been performed on this layout to try to make the most efficient use of the space. Constraints include the size of the rf cavities, which is dictated by the frequency, the size of the absorbers, which is determined by the beam size, and the cell length, which has been fixed for this Study at 2.75 m for the buncher and Lattice 1 cooling section and 1.65 m for the Lattice 2 cooling section. The two lattice cell dimensions will be re-evaluated as part of the overall system optimization.

The sizes of the coil packs and cryostats have been chosen to allow practical current densities and the coil diameters have been kept small to minimize the amount, and therefore the cost, of superconductor required. The largest coil is the central one (“coupling coil”) that surrounds the rf cavities. The inner diameter of this coil is left large enough to allow the cavity structures to pass through during assembly. The rf feeds must come out through the wall of the cryostat, and may be angled to give clearance to other hardware. Pumping ports will be short and wide to give good conductance and may also penetrate the cryostat. Clearance is required at the end of each cooling cell for installation or removal of one absorber/rf module from the channel. This is achieved by using a collapsible flange in the outer cryostat wall, which is reinforced after it is made up in order to handle the possible magnetic forces. RF shields will be used to keep beam-induced signals from escaping into the outer cryostat and vacuum system.

Figure 8.20 shows the proposed cooling channel layout for the first cooling section lattice, including all major components except the beam instrumentation package, which will occupy the clearance opening at the end of each cell or, possibly, the space between the rf cavities and the hydrogen absorber. The space in the cryostat outside of the cavities will be evacuated to minimize the load on the rf structures. This approach would provide insulation for the cavities if they were operated below room temperature. It also obviates the need for UHV connections between each cavity and between the cavities and the hydrogen absorbers. The flanges are required only to provide rf continuity (for screening) and to separate the UHV of the rf system from the guard vacuum of the cryostat.

8.4.4 1.65 m Lattice Implementation (Lattice 2)

The 1.65 m lattice for the downstream part of the cooling channel will use a layout similar to the upstream part, but with smaller hydrogen absorbers and only two rf cavities per

8.4. Specification of NCRF Cavities for Cooling

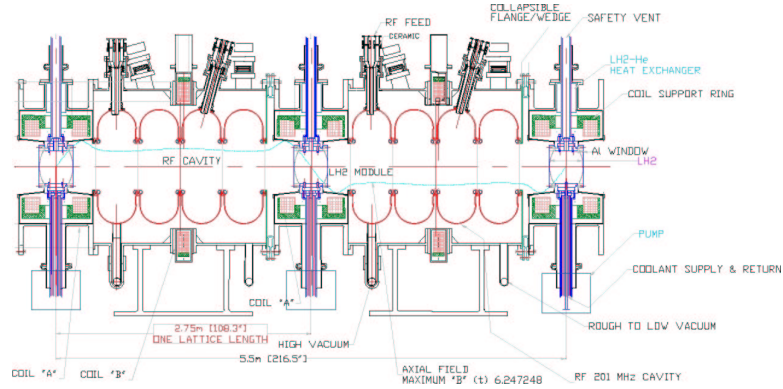


Figure 8.20: Cooling channel Lattice 1, four cavities per cell.

cell. The density of equipment is similarly high. In this case the cavity lengths are closer to the optimum for this particle velocity, but could still be improved if the cell length were increased slightly. Figure 8.21 shows the proposed cooling channel layout for lattice 2, including all major components except the instrumentation package.

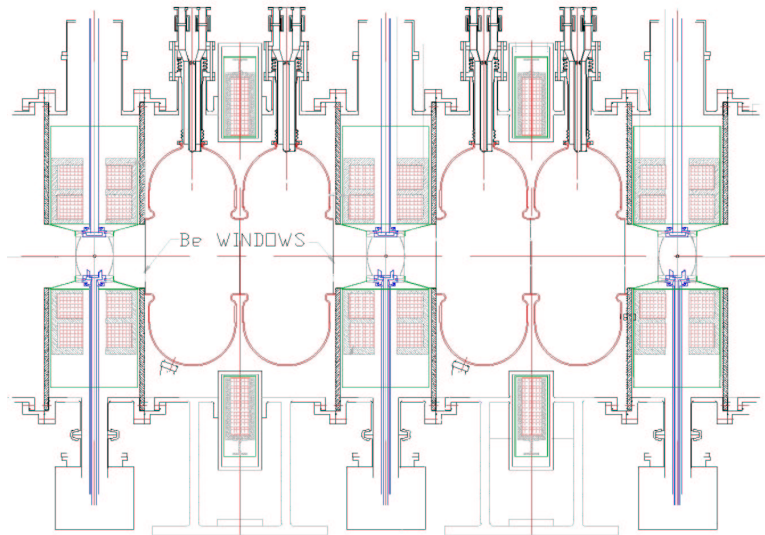


Figure 8.21: Cooling channel Lattice 2, two cavities per cell.

8.4.5 402.5 MHz Buncher Cavity

The buncher harmonic cavities, Fig. 8.22, are smaller, simpler versions of the 201.25 MHz cavities. They are rounded pillboxes and are closed by similar foils that are smaller and thinner than those used for the large cavities. There is adequate space for the cavities to be the optimal length for this particle velocity. Though the power requirements are modest, cooling water is used to stabilize the frequency and remove the small amount of average power dissipated in the walls. Harmonic cavities are installed in some of the buncher cells in the location corresponding to that where the hydrogen absorbers are placed in the normal cooling sections, *i.e.*, inside the bore of the focusing solenoid coils.

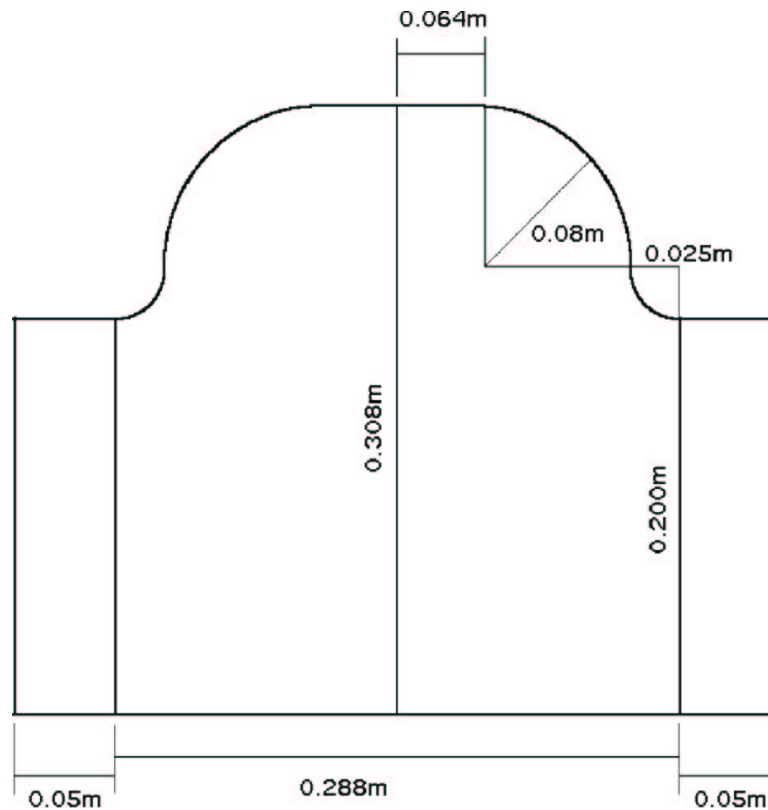


Figure 8.22: 402.5 MHz buncher harmonic cavity.

8.4. Specification of NCRF Cavities for Cooling

8.4.6 Tuning Requirements

Since there is negligible beam loading, the tuning requirement for the cavities is simply to compensate for temperature variations due to water supply changes and rf heating. If we assume bulk water temperature fluctuations are of the order of 1°C or less, and a thermal expansion coefficient of copper of approximately $17\text{ ppm}/^\circ\text{C}$, then the frequency variation would be about 3.4 kHz . Since the average power is modest, it should be easy to limit the temperature rise due to rf heating to 10°C or less. A worst-case cold start with the cavities around 0°C and a normal operating temperature of 40°C would produce a frequency detuning of about 136 kHz . Simple 2D calculations show that if the length of the cavity is varied from the nominal value, the frequency sensitivity is about 236 kHz/mm , so a small range of motion would be adequate to achieve the required tuning range. A tuning scheme similar to that used for superconducting cavities, where the cavity is mechanically stretched or compressed within elastic limits, will easily achieve this range of motion. Alternatively, a moving plunger tuner can be used to tune the cavity inductively but this would require an additional aperture in the cavity and would be harder to package within the confines of the cryostat.

It would also be possible to tune the cavities over a limited range by controlling the water temperature, but the water stability would have to be a fraction of a degree to keep the frequency stable to within the bandwidth of the cavity (3.3 kHz unloaded, 6.6 kHz critically coupled). Moreover, each cavity would then require an independent water circuit and controller, which would be inconvenient.

Depending on the elastic range of motion of the cavities, it may be desirable to have some kind of *fixed* tuning after assembly to account for manufacturing tolerances (analogous to the “dimpling” of linac cavities). This could be a specific part of the cavity which is designated to be deformed or the cavity as a whole could be designed such that it can be stretched or compressed beyond the elastic limit to achieve a permanent tuning. If detailed analysis shows that the cavity has a sufficiently large elastic tuning range, it may even be possible to relax the requirement of keeping the foils flat and allow some movement to take place. (Pre-bowing of the foils would ensure that this happens in a predictable manner.) This would allow thinner foils to be used with a concomitant reduction in scattering.

In the event that vibrations of the foils or other parts of the system should produce troublesome fluctuations in the rf fields, the deforming type tuner could be augmented with a fast piezo-electric actuator allowing feedback at audio frequencies. This has been demonstrated to reduce the effect of microphonics in superconducting cavities.

8.4.7 Vacuum Requirements

The operating vacuum in the high-gradient cavities should be in the 10 nTorr range or better. Operating much above this range is likely to produce more frequent arcing and would require significantly longer time to condition the cavities initially and after any vent. The reliability of the rf window is also strongly influenced by the vacuum level. The frequency of window arcs and the lifetime of anti-multipactor coatings on the ceramic are both degraded by operating at pressures above about 100 nTorr. These conditions will require strong pumping and good conductance to the rf cavities. Because of the presence of strong solenoid magnetic fields, ion pumps may not be used in close proximity to the cavity during operation, though they may be useful during initial conditioning with solenoids off. Cryopumps or titanium sublimation pumps may be useful close to the cavities with magnetic fields on. It would be advantageous to pump the cavities through the rf coupler if there proves to be sufficient conductance, since this will ensure the best possible vacuum at the rf input window. A large diameter coaxial feed with a short distance to the pump may have sufficient conductance by itself. If not, it can be supplemented by an additional pumping port on the cavity body. A thorough bakeout to above 150°C after assembly would be advantageous but may be incompatible with the superconducting components. In that case, the individual components will be baked separately before final assembly into the cryostat.

8.5 SCRF Cavities for Acceleration

Based on the high-real estate gradient desired to minimize muon loss, superconducting cavities are selected for the acceleration section of the Neutrino Factory to provide an active gradient of 15-17 MV/m, and a real-estate gradient of 7.4 MV/m. At such high-gradients, the peak rf power demand for copper cavities that provide 7.5 GV would become prohibitively expensive. By virtue of low losses, SC cavities can be filled slowly, reducing the peak power demand to roughly 0.5 MW per cell for a 3 ms rise time.

As a result of experience at LEP, CEBAF, TTF, Cornell, KEK and CEA-Saclay, the science and technology of superconducting cavities and associated components are highly developed [6]. In all, SCRF systems totaling 1 km in active length have been installed in a variety of accelerators and routinely operated to provide a total of 5 GV. The largest installation was at LEP-II, where 500 m of niobium-coated copper cavities provided more than 3 GV of acceleration [7]. The Neutrino Factory calls for nearly 500 m to provide 7.4 GV.

Although the sheet-metal Nb cavities used for TESLA are capable of providing gradi-

8.5. SCRF Cavities for Acceleration

ents of the order of 20 MV/m and higher [8], we have chosen Nb/Cu technology, developed at CERN [9] for LEP-II, for several reasons:

- Because of the low rf frequency (201.25 MHz), and the accompanying thicker wall (*e.g.*, 6 mm), the cost of raw sheet niobium would be prohibitive for the roughly 600 cells needed.
- High thermal conductivity copper provides better stability against quenching of superconducting cavities than does sheet Nb. This is especially beneficial at 201.25 MHz because of the high stored energy per cell (roughly 1 kJ per cell at design gradient).
- The wall thickness of 201.25 MHz cavities may need to be even greater than 6 mm for mechanical stability against atmospheric load, for reducing Lorentz force detuning, and for avoiding microphonics from external vibrations.
- A coated copper cavity allows the use of pipe cooling instead of the more usual bath cooling. Pipe cooling saves liquid-helium inventory (estimated at 100,000 L for standard bath cooling of 600 cells). It also opens additional avenues for improving the mechanical stability for large scale cavities.

Recent results from CERN [10] on 400 MHz Nb/Cu cavities (Fig. 8.23) demonstrate accelerating gradients of 15 MV/m at 2.5 K at a Q of 2×10^9 . Because of the lower frequency used here, we can expect the Q to be four times higher. We have chosen an operating temperature of 2.5 K and a Q value of 6×10^9 . Extrapolating LEP results at 4.5 K would imply a much lower $Q < 2 \times 10^9$ at the design gradient for the Neutrino Factory, even when scaled for the lower frequency. Moreover, LEP cavities never reached the Neutrino Factory design gradients at 4.5 K.

Modeling the Q vs. E (Fig. 8.24) obtained for LHC 400 MHz cavities and incorporating the Q increase for 201.25 MHz, ANSYS studies conclude that it will not be possible to reach $E_{acc} = 15\text{--}17$ MV/m at a Q of 6×10^9 , unless the operating temperature is reduced to 2.5 K. Figure 8.24 shows the peak magnetic field expected for 17 MV/m in a 2-cell cavity with 300 mm beam aperture. It corresponds to $E_{acc} = 13$ MV/m for the LHC cavity geometry because of the relatively smaller beam pipe and optimized cavity. (The Neutrino Factory cavity geometry is discussed below.)

Accelerator physics studies show that an aperture of 300 mm (diameter) is acceptable for the Neutrino Factory, except for the first 1000 MeV of the pre-accelerator linac, where an aperture of 460 mm has been chosen. Because of the higher peak fields arising from the larger aperture, the gradient for the first section of the pre-accelerator has been reduced

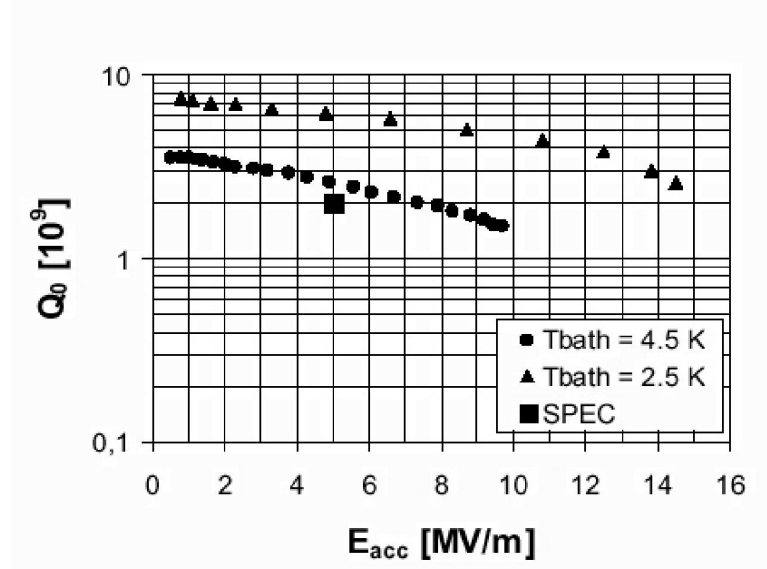


Figure 8.23: Q_0 vs. gradient for Nb/Cu CERN 400 MHz, LHC cavity.

to 15 MV/m. The corresponding surface magnetic field is still 12% less than the peak magnetic field for the LHC cavity at 15 MV/m.

In selecting the rf pulse length (T_{rf}), a trade-off must be made between peak rf power on the one hand, and refrigerator load, tolerance to microphonics and Lorentz force (LF) detuning on the other hand. Increasing T_{rf} will lower the peak power, but increase the average rf power and the refrigeration load. Increasing T_{rf} will also drive Q_L toward higher values, decreasing the cavity bandwidth and thereby increasing its sensitivity to LF detuning and microphonics. The peak rf power (P_{pk}) needed to establish the fields depends on the stored energy (U), the cavity time constant ($\tau = \frac{Q_L}{\omega}$) and the amount of detuning $\delta\omega$ expected from Lorentz force and microphonics, as follows [6]

$$P_{pk} = \frac{U \left(\frac{\omega}{Q_L} \right) \left\{ (Q_L \frac{\delta\omega}{\omega})^2 + \frac{1}{4} \right\}}{\left\{ (1 - \exp - \frac{T_{rf}}{2\tau}) \right\}^2} \quad (8.1)$$

Once the fill time and detuning tolerance are selected, the loaded Q of the cavity can be found to minimize the peak power required. A conservative estimate for detuning tolerance in these large 201.25 MHz structures is 40 Hz. Cavities at TTF and CEBAF show microphonic excitation of < 10 Hz [11]. For a fill time of 3 ms, the optimum Q_L

8.5. SCRF Cavities for Acceleration

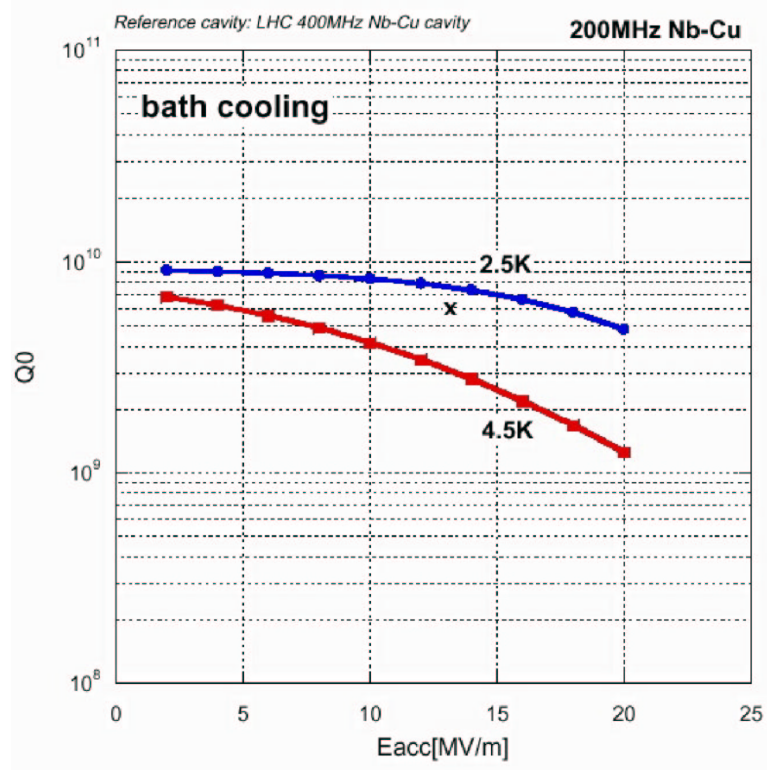


Figure 8.24: Q_0 vs. gradient expected for 201.25 MHz cavity. Although the Neutrino Factory design is $Q_0 = 6 \times 10^9$ at $E_{acc} = 17$ MV/m, for a 2-cell, 300 mm aperture cavity, it corresponds to only 13 MV/m (marked X) for the LHC cavity geometry due to the smaller aperture of this cavity and the optimized geometry.

is 1×10^6 (bandwidth = 200 Hz) and the required peak power is about 500 kW per cell. Coaxial couplers developed for KEKB [12] have delivered 380 kW CW to a 1 A beam. In pulsed mode, higher power performance is expected. For a wall thickness of 8 mm, the calculated Lorentz force detuning at 17 MV/m is 128 Hz. Most of this can be handled with feed-forward techniques developed at TTF for TESLA [13].

8.5.1 SCRF Structures at 201.25 MHz

To improve the real-estate gradient, it is important to have a large filling factor of cavities in the cryomodule. This pushes structures towards multi-cell cavities. On the other hand, because of the low frequency and high-gradient, the coupler power and stored energy per structure increase with the number of cells. Also, the mechanical resonance frequency of multi-cell cavities drops, demanding stiffening schemes. Compromising between these factors, 2-cell units are chosen. In the first 1000 MeV of the preaccelerator linac, where apertures of 460 mm are needed, gradients are lowered to 15 MV/m to keep the peak surface fields comparable to those of the 300-mm bore cavity at 17 MV/m; input coupler power is kept at the 500 kW level by providing one coupler at each end. The performance

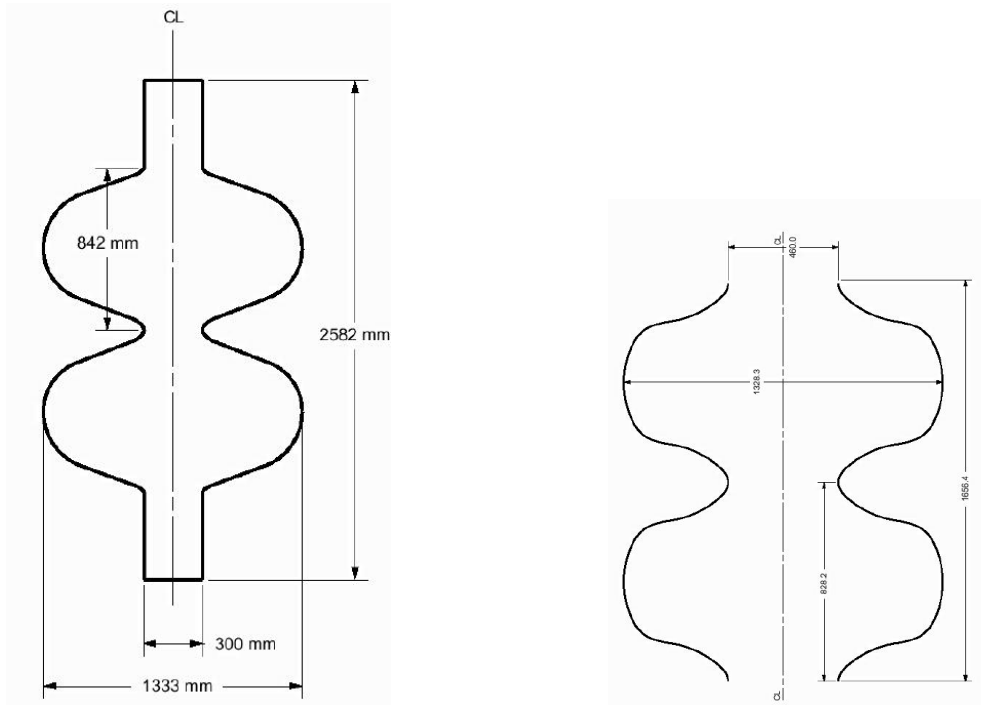


Figure 8.25: Two-cell geometry: (left) small aperture; (right) large aperture.

of a superconducting cavity depends on the peak surface fields. Minimizing E_{pk} is important to avoid field emission that lowers the cavity Q and increases heat load. Minimizing H_{pk} is also important, since the Q of these cavities falls with surface magnetic field, one of the characteristic features of Nb/Cu cavities (Fig. 8.23). In the 400 MHz LHC cavity, which reached $E_{acc} = 15$ MV/m, the corresponding peak surface fields were $E_{pk} = 33$

8.5. SCRF Cavities for Acceleration

MV/m and $H_{pk} = 750$ Oersted. The LHC cavity has a beam pipe diameter of 300 mm. Keeping the same beam pipe diameter for 201.25 MHz, 2-cell cavities, it is possible to improve the Neutrino Factory cavity geometry (see Fig. 8.25) to reduce the peak fields to 14% below LHC-cavity values. Relative to CERN cavity performance, there is adequate safety margin for both improved structure choices. Tables 8.6 and 8.7 list the properties of the 2-cell 300 mm aperture unit and the 2-cell large aperture unit, respectively. Figure 8.25 (left panel) shows the 2-cell geometry with 300 mm aperture and (right panel) shows the 2-cell geometry with 460 mm aperture. Figure 8.26 shows the deformation (exaggerated) due to Lorentz force detuning for the 2-cell, 300 mm diameter cavity.

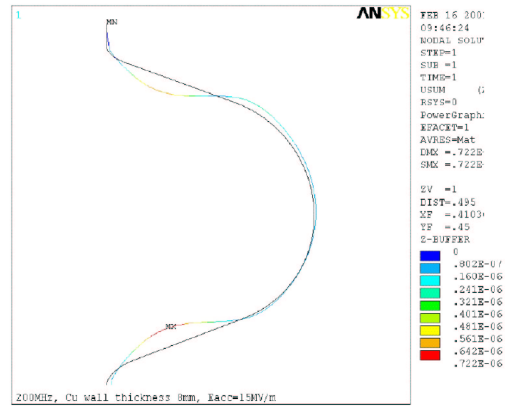


Figure 8.26: Lorentz force detuning for 8 mm wall thickness cavity.

8.5.2 Input Power Coupler

The antenna type coaxial design was chosen based on the successful experiences of CERN (LEP-II), DESY (HERA and TTF) and especially the success of the input coupler for KEKB [12]. Figure 8.27 shows the dimensions of the KEK, 508 MHz coupler, which will be scaled proportionately to 201.25 MHz. The lengths of the various sections will be adjusted to fit the final cavity and cryostat designs adopted. The waveguide-to-coaxial transition is of the door-knob variety. As in all high-power applications, the main window will be at room temperature and remote from the cavity. At KEKB, it is a disk shaped, water cooled, 95% pure alumina ceramic with a central hole for the inner conductor. A teflon coaxial centering disk between the window and doorknob serves to limit the flow of air to the cavity in the unlikely event of a ceramic window break. The inner conductor is

8.5. SCRF Cavities for Acceleration

Table 8.6: 2-cell, 300 mm-diameter cavity parameters.

RF freq (MHz)	201.25
No. of cells per cavity	2
Active cavity length (m)	1.5
No. of cavities	268
Linac	76
RLA	192
Aperture diameter (mm)	300
E_{acc} (MV/m)	17
Energy gain per cavity (MV)	25.5
Stored energy per cavity (J)	2008
R/Q (Ω /cavity)	258
E_p/E_{acc}	1.43
H_p/E_{acc} (Oe/MV/m)	38
E_{pk} at 17 MV/m (MV/m)	24.3
H_{pk} at 17 MV/m (Oe)	646
Q_0	6×10^9
Bandwidth (Hz)	200
Input power per cavity (kW)	1016
RF on-time (ms)	3
RF duty factor (%)	4.5
Dynamic heat load per cavity (W)	18.9
Operating temperature (K)	2.5
Q_L	10^6
Microphonics detuning tolerable (Hz)	40
Wall thickness (mm)	8
Lorentz force detuning at 15 MV/m (Hz)	128

made of OFHC copper pipe and is water cooled. The outer conductor is made of copper plated (30 mm) stainless steel and has fins cooled by a 4.5 K stream from the refrigerator. This reduces both the dynamic and static heat leaks associated with the coupler.

Benefiting from simulation codes recently available for calculating and avoiding multipacting [14], dimensions of the inner and outer conductors are chosen so that multipacting will not be a serious problem. The coaxial design also permits application of a DC bias voltage between the two conductors to curtail any possible multipacting that may develop near the window or other sensitive regions.

8.5. SCRF Cavities for Acceleration

Table 8.7: 2-cell, 460 mm-aperture cavity parameters.

RF freq (MHz)	201.25
No. of cells per cavity	2
Active cavity length (m)	1.5
No. of cavities	43
Aperture diameter (mm)	460
E_{acc} (MV/m)	15
Energy gain per cavity (MV)	22.5
Stored energy per cavity (J)	1932
R/Q (Ω /cavity)	208
E_p/E_{acc}	1.54
H_p/E_{acc} (Oe/MV/m)	44
E_{pk} at 15 MV/m (MV/m)	23.1
H_{pk} at 15 MV/m (Oe)	660
Q_0	6×10^9
Bandwidth (Hz)	200
Input power per cavity (kW)	980
RF on-time (ms)	3
RF duty factor (%)	4.5
Dynamic heat load per cavity (W)	18.3
Operating temperature (K)	2.5
Q_L	10^6
Microphonics detuning tolerable (Hz)	40

The coupler will be equipped with standard diagnostics for vacuum, gas species, temperature and light monitoring. Vacuum and light levels can be used to trip the rf power source in case of arcs.

The Q_{ext} value of the input coupler is fixed after initial adjustment of the position of the inner conductor by the use of appropriate spacing washers during final assembly. From experience at KEK, we expect that the Q_{ext} for the non-accelerating modes of the fundamental pass band will be of the same order as the Q_{ext} for the accelerating mode, *i.e.*, a few $\times 10^5$.

8.5.3 Higher-Order Mode (HOM) Couplers

The function of the HOM couplers is to damp the higher-order modes to Q_{ext} values of $10^4 - 10^5$ to prevent resonant build up of beam-induced fields that may make the beam unstable or increase the HOM power. The HOM couplers extract beam-induced HOM power from the cavity and deposit it in room-temperature loads. In view of the large muon bunch length, we do not expect HOMs to be a serious issue.

Two couplers are needed, with a relative azimuthal angle of about 90° to ensure damping of both polarizations of dipole modes. One coupler is attached to each end of the cavity. The HOM couplers must reject the accelerating mode by means of a narrow-band filter built into the coupler.

Detailed calculations will be carried out during the prototyping stage for the HOM spectra, possible trapped modes, and expected HOM power. Codes exist and procedures have been well established for electron applications. Our baseline device is a loop type coupler (Fig. 8.28) because it is demountable, compact, has relaxed mechanical tolerances, and provides demonstrated performance in mode damping [15]. The plane of the loop is orthogonal to the beam axis. The loop couples mainly to the magnetic field of dipole modes and mainly to the electric field of longitudinal modes. The rejection filter is formed by the inductance of the loop and the capacitance between the loop end and the outer conductor. The loop is capacitively coupled to the external load via a type-N connector, and is cooled by conduction through an upper stub. Final tuning of the filter can be carried out outside the clean room once the coupler is attached and the cavity sealed. Q_{ext} values are typically 10^3 to 10^5 for high impedance modes in a 9-cell TESLA cavity. These Q value will be even lower for the 2-cell cavities.

Power tests carried out for TESLA cavities under CW operating conditions showed good thermal behavior up to an accelerating field of 21 MV/m.

8.5. SCRF Cavities for Acceleration

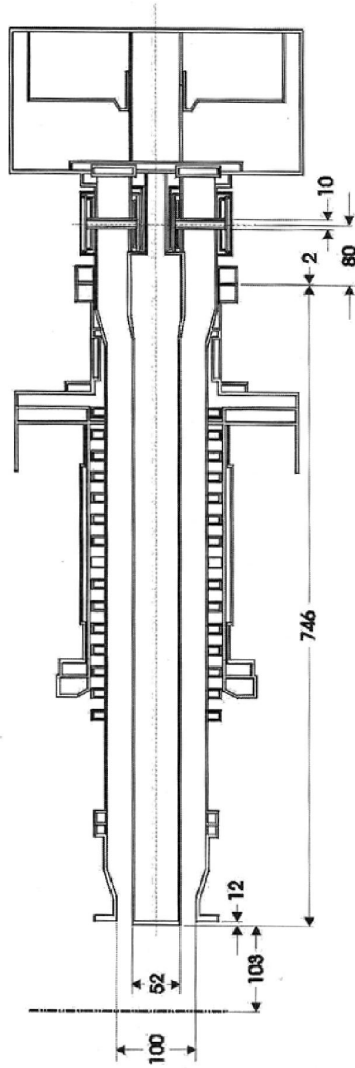


Figure 8.27: KEKB 508-MHz coupler.

8.5.4 Tuner

The function of the tuner is to match the cavity resonance frequency to the desired accelerator operating frequency. If the cavity is not being used for acceleration, the tuner must detune the cavity frequency a few bandwidths away from resonance, so that the beam will not excite the fundamental mode. During accelerator operation, the tuner

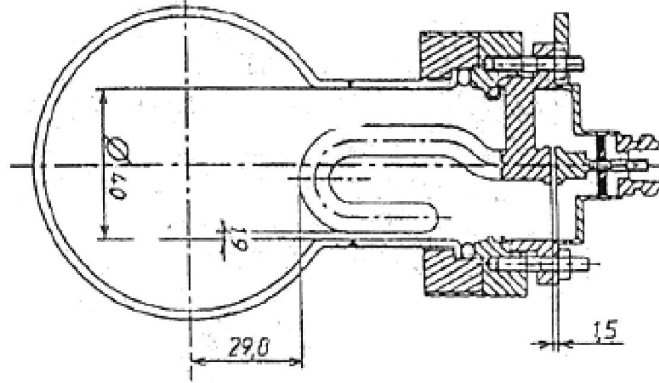


Figure 8.28: TESLA-type HOM coupler.

must correct for slow changes in the cavity frequency due to changes in the liquid-helium bath-pressure, or in the lengths of the cavity and He vessel support system. Tuning is achieved by varying the total length of the cavity within its elastic limit, so that the field flatness is preserved. The tuning coefficient of a 2-cell cavity is of the order of 50 Hz/mm. (Plunger tuners are not advisable in superconducting cavities because of moving parts and the danger of dust.)

With a mechanical tuner, the length of the cavity is controlled by an electromechanical system acting differentially with respect to the cavity body. If each cavity is enclosed in its own helium vessel, the latter must have some flexibility built in.

A mechanical tuning system is generally composed of a stepping motor, a gear box, a screw and nut assembly, and a lever arm with a flex mechanism attached. A fast piezoelectric element can be added for fine tuning, compensating Lorentz force detuning, Fig. 8.26, as well as microphonics. Figure 8.29 shows the lowest frequency vibrational mode of the two-cell cavity that could be excited by vibrations. The stiffness will be increased to raise the frequencies of this and other mechanical modes.

Alternatively a thermal tuner could be considered, modeled after the LEP system [16]. This uses three Ni tubes as tuner bars located in the cryomodule insulation vacuum. The tuner rib cage can also help increase the mechanical resonant frequency of cavity longitudinal modes. For slow tuning in one direction (constriction) the temperature of the tubes is lowered by flowing cold helium gas. For tuning in the opposite direction the temperature is raised by centrally located electric heaters. The typical tuning speed is 10 Hz/sec. Heat losses are minimized by counter-flowing cold He gas through the tuner

8.5. SCRF Cavities for Acceleration

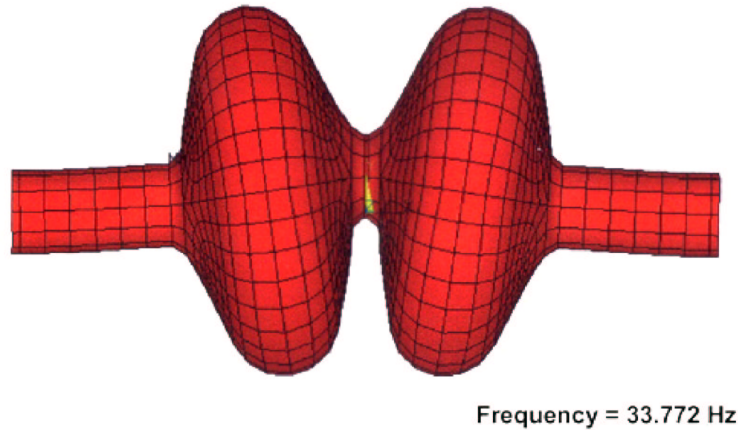


Figure 8.29: Lowest vibrational mode of 2-cell cavity.

tubes. For fast tuning, coils can be wound around the Ni tubes to produce a magnetic field that changes the length of the tubes by the magnetostrictive effect. Rapid (ms) tuning ranges of kHz are possible.

Tuners are an active part of the complete rf low-level control system, which stabilizes the frequency, amplitude and phase variations induced by sources such as the rf drive, beam current variations, Lorentz force detuning, and microphonics.

8.5.5 Cryogenics for SCRF

Figure 8.30 shows a 3D CAD model of the long cryomodule with four 2-cell units and a focusing magnet. Each cavity has two input couplers, one on each end, and two HOM couplers, also one on each end. Mature cryomodule designs (see Fig. 8.31), available at CERN for LEP-II and LHC will be adapted to the Neutrino Factory needs. Based on scaling from LEP 12.5-m long cryomodules, 4.5 K static heat leaks of 100 W per cryomodule are expected. Thin beryllium windows will be placed on the beam line at each end of the cryomodule to protect the cavity vacuum and to keep the cavity surfaces clean during installation into the beam line. Tables 8.8, 8.9 and 8.10 give cryomodule parameters. Table 8.11 gives a summary for the total SCRF requirements. The hardware implementation of the refrigerator is described in Chapter 11.

8.5. SCRF Cavities for Acceleration

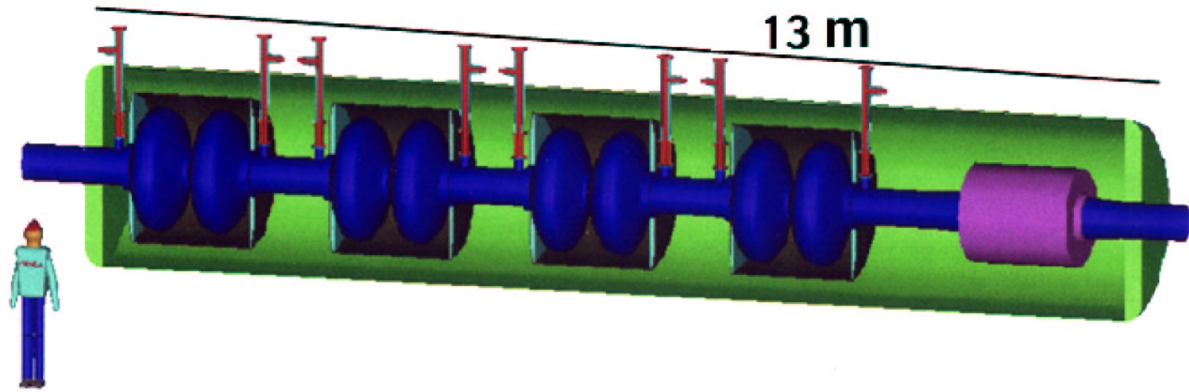


Figure 8.30: Long cryomodule.



Figure 8.31: LEP cryomodule.

8.5. SCRF Cavities for Acceleration

Table 8.8: Short cryomodule parameters.

No. of cryomodules (in linac)	11
No. of 2-cell cavities in one cryomodule	1
No. of input couplers	2
Overall length (m)	5
Active length (m)	1.5
Cavity dynamic heat load at 2.5 K (W)	18
Couper dynamic heat load at 2.5 K (W)	1
Coupler static heat load at 2.5 K, 5–8 K, 40–80 K (W)	2, 4, 40
Cryomodule static heat load at 2.5 K, 5–8 K, 40–80 K (W)	6, 60,600
Total 11 cryomodule heat load @ 2.5 K, 5–8 K, 40–80 K (W)	300, 700, 7000

Table 8.9: Intermediate cryomodule parameters.

No. of cryomodules (in linac)	16
No. of 2-cell cavities in one cryomodule	2
No. of input couplers	4
Overall length	8 m
Active length	3 m
Cavity dynamic heat load at 2.5 K (W)	36
Couper dynamic heat load at 2.5 K (W)	2
Coupler static heat load at 2.5 K, 5–8 K, 40–80 K (W)	4, 8, 80
Cryomodule static heat load at 2.5 K, 5–8 K, 40–80 K (W)	7, 70, 700
Total 16 cryomodule heat load at 2.5, 5–8 K, 40–80 K	790, 1250, 12,500

8.5.6 Power Source for SCRF

The superconducting linac and recirculating linear accelerator (RLA) designs employ a total of 311 cavities. The linac contains 119 cavities running at a gradient of up to 17 MV/m. (The early part of the linac operates at a gradient of 15 MV/m). The rf pulse length is 3 ms and the average repetition rate is 15 Hz, although the recovery time between pulses is only 20 ms. Each cavity is driven by two 500 kW couplers. With a 20% rf power overhead, this works out to 1.2 MW per cavity and a total rf requirement of 375 MW.

Examination of the average power requirement demonstrates that a very high efficiency source is required. The best candidate for the required source is again a multi-

8.5. SCRF Cavities for Acceleration

Table 8.10: Long cryomodule parameters.

No. of cryomodules (19 linac + 48 RLA)	67
No. of 2-cell cavities in one cryomodule	4
No. of input couplers	8
Overall length (m)	13
Active length (m)	6
Cavity dynamic heat load at 2.5 K (W)	$4 \times 19 = 76$
Couper dynamic heat load at 2.5 K (W)	$8 \times 0.5 = 4$
Coupler static heat load at 2.5 K, 5–8 K, 40–80 K (W)	8, 16, 160
Cryomodule static heat load at 2.5 K, 5–8 K, 40–80 K (W)	10, 100, 1000
Total 67-cryomodule heat load at 2.5 K, 5–8 K, 40–80 K (kW)	6.6, 7.8, 78

Table 8.11: SCRF overall parameters for a Neutrino Factory.

No. of cryomodules	94
No. of 2-cell cavities	311
No. of input couplers	622
Overall length (m)	1054
Active length (m)	467
Filling factor	0.44
Total voltage (GV)	7.5
Average real estate gradient (MV/m)	7.8
Total heat load at 2.5 K, 5–8 K, 40–80 K (kW)	7.7, 9.7, 94
Cryo load (with $\times 1.5$ safety factor) 2.5 K, 5–8 K, 40–80 K (kW)	11.6, 14.6, 141
Assuming efficiency multipliers of 600, 225, 20	
AC power for refrigeration (MW)	13
Total peak rf power (with 20% margin for control/losses)(MW)	362
Average rf power (MW)	16.3
AC power for rf (efficiency multiplier = 2) (MW)	35.6
Total AC power (MW)	49

beam klystron (MBK). This could be the same basic design as that used for the NCRF system but with increased thermal capacity to handle the increased duty factor. Thompson has developed a 7-beam MBK with an efficiency near 70%, see Section 8.3.1 and reference [2]. Scaling this design to 201.25 MHz would produce a 5 MW, 19 beam MBK

8.6. Conclusions

with each beam having a perveance of 5×10^{-5} . The tube, with gun and collector, would be about 5.7 m in length and could be manufactured by industry after some initial R&D. A 37-beam MBK has also been developed by other groups [5].

Each tube will drive four cavities through 8-way power splitters. The specifications for the modulator, an IGBT-type like that described in Section 8.3.3 for the NCRF, are 50 kV at 142 A, with an average power of 320 kW. To save costs, the modulator will be designed to operate two 5 MW tubes, requiring twice the current and average power rating. A total of 78 tubes and 39 modulators are required to supply the rf power requirements. The multi-beam klystron may be designed with a vapor-cooled collector to save on the cooling water requirement. Such a system is at least ten times more efficient than conventional water cooling. With vapor cooling, each tube will require 120 gpm of near-room-temperature cooling water with a total installed capacity of 9,360 gpm. Assuming an efficiency of 95%, each modulator station will require 694 kW of installed AC power for a total of 27 MW.

8.6 Conclusions

The normal conducting and superconducting systems have continued to evolve since Study-I. Both cavity designs have been studied in some detail and feasible solutions have been developed for the required cooling channel and acceleration parameters. Ongoing R&D programs are addressing the practical aspects of cavity fabrication and conditioning. The cooling channel layout, though densely packed, has shown the feasibility of assembling all of the vital components. There is room for further optimization of the cooling channel, notably by adjusting the total cell length, to reduce the rf power requirements and reduce the superconducting magnet costs. The superconducting rf accelerating section has been developed using design choices that are consistent with the state of the art at various laboratories around the world.

Bibliography

- [1] Daryl W. Sprehn, *MBK Calculations*, Feb 26, 2001; N. Holtkamp and D. Finley, eds., *A Feasibility Study of a Neutrino Source Based on a Muon Storage Ring*, Fermilab-Pub-00/108-E (2000), Chapter 10, p. 10-17, and 19.
<http://www.fnal.gov/projects/muon-collider/nu-factory/nu-factory.html>
- [2] A. Beunas, G. Faillon, THOMSON TTE, France, S. Choroba, A. Gamp, DESY, Germany *A High Efficiency Long Pulse Multi Beam Klystron For The Tesla Linear Collider*, Submitted to PAC 2001.
- [3] R.A. Rimmer, N. Hartman, D. Li, Al. Moretti, T. Jurgens *Closed-Cell 201.25 MHz rf Structures for a Muon Cooling Channel*, submitted to PAC 2001.
- [4] N. Hartman, D. Li, J. Corlett, *Thin Beryllium Windows - Analysis and Design Status*, <http://www-mucool.fnal.gov/mcnotes/muc0180.pdf>.
- [5] A. Larionov, International Workshop on Pulsed RF Sources For Linear Colliders (RF93), July 5-9, 1993, Dubna-Protvino, Russia.
- [6] H. Padamsee, J. Knobloch and T. Hays, *RF Superconductivity for Accelerators*, John Wiley and Sons, 1998.
- [7] P. Brown et al., *Proceedings of the 9th Workshop on rf Superconductivity* (1999) ed. by B. Rusnak, p. 1.
- [8] D. Proch, *Proceedings of the 9th Workshop on rf Superconductivity* (1999) ed. by B. Rusnak, p. 19 and D. Trines., *ibid.*, p. 605.
- [9] E. Chiaveri, *Proceedings of the 1996 European Particle Accelerator Conference*, ed., S. Myers et al., Barcelona, Spain, IOPP Publishing, Bristol, p. 200 (1996).
- [10] E. Chiaveri, *Proceedings of the 9th Workshop on rf Superconductivity* (1999) ed. by B. Rusnak, p. 352. and S. Bauer et al., *ibid.* p. 437.

BIBLIOGRAPHY

- [11] C. Reece, *Proceedings of the 8th Workshop on rf Superconductivity*, ed. by V. Palmieri and A. Lombardi (1998) p. 138.
- [12] T. Furuya et al., *Proceedings of the 9th Workshop on rf Superconductivity* (1999) ed. by B. Rusnak, p. 31.T; and S. Mitsunobu, *ibid.* p. 505.
- [13] S. Simrock et al., *Proceedings of the 9th Workshop on rf Superconductivity* (1999) ed. by B. Rusnak, p. 92.
- [14] E. Somersalo et al., *Proceedings of the 1995 Particle Accelerator Conference*(1996), Dallas Texas, p. 1623.
- [15] J. Sekutowicz, TESLA Note, 94-07 (1994).
- [16] G. Cavallari et al., *Proceedings of the 3rd Workshop on rf Superconductivity* (1988) ed. by K. Shepard, p. 625.